

High Mass X-ray Binary Pulsars in the Small Magellanic Cloud

W.A.Majid

Jet Propulsion Laboratory, California Institute of Technology, Pasadena, CA 91109

R.C.Lamb

Space Radiation Laboratory, California Institute of Technology, Pasadena, CA 91125

D.J.Macomb

Physics Department, Boise State University, Boise, ID 83725-1570

ABSTRACT

We report two additions to the class of accreting X-ray pulsars from the direction of the Small Magellanic Cloud with periods of 263 and 202 s. (Recently Haberl & Pietsch (2004) reported the 263 s pulsar.) The source positions of these two pulsars are consistent with early B stars in the SMC and therefore we identify them as high mass X-ray binaries (HMXBs). Properties of an ensemble of 24 optically identified HMXB pulsar from the SMC are investigated. The locations of the pulsars and an additional 14 X-ray pulsars not yet identified as having high mass companions are located predominately in the young ($\text{ages} \leq 3 \times 10^7$ years) star forming regions of the SMC as expected on the basis of binary evolution models. We find no significant difference between the distribution of spin periods for the HMXB pulsars of the SMC compared with that of the Milky Way. For those HMXB pulsars which have Be companions we note an inverse correlation between spin period and maximum X-ray flux density. This correlation may be a reflection of the fact that the spin periods and orbital periods of Be HMXBs are correlated. We note a similar correlation between X-ray luminosity and spin period for the Be HMXB pulsars of the Milky Way. We have also established the pulse period of the possible AXP CXOU J010043.1-721134 to be 8.0 s. This corrects an earlier report (Lamb et al. 2002b) of a 5.4 s period for this object

Subject headings: — galaxies: individual (SMC) — pulsars: general — stars: neutron — X-rays: stars

1. Introduction

X-ray binaries are conventionally divided into two distinct classes: high mass (companion stars with masses ≥ 8 solar masses) and low mass (companion masses ≤ 1 solar mass) with relatively

few X-ray binaries having companions with masses in the intermediate range. The division into the two classes makes sense, since their evolution is quite different. For the high mass binaries, the maximum lifetime for their existence is set by the nuclear burning time of an 8 solar mass star, which is $\sim 3 \times 10^7$ yr (Verbunt & van den Heuvel 1995). Whereas low-mass X-ray binaries have lifetimes of 10^{8-9} yr or more. This characteristic of the HMXBs makes them a useful measure of recent star forming activity in galaxies (see for example: Grimm et al. 2003).

From an observational point-of-view the advantages of studying the compact object content of the Magellanic Clouds are well known: a relatively small angular size, at a reasonably close and known distance, located at a high galactic latitude with little obscuration by the interstellar medium of the Galaxy. In addition, there is evidence for recent star formation in the SMC at a level far in excess of either the Milky Way or the LMC.

The HMXB population of the Small Magellanic Cloud has recently been catalogued by Liu et al. (2000). Since then two papers have reported on the X-ray population of the SMC based on specific X-ray satellite data. Yokogawa et al. (2003) summarizes source populations bases on ASCA data; Sasaki et al. (2003) on the basis of *X-ray Multi-Mirror Mission–Newton* satellite data.

In this paper we report the discovery of two X-ray pulsars from the direction of the SMC, having periods of 202 and 263 s, using data from the *X-ray Multi-Mirror Mission–Newton* satellite. The 263 s pulsar has recently been reported by Haberl & Pietsch (2004). Both pulsars are sufficiently close to high mass companions that the association is likely. These discoveries continue our program of routinely evaluating the pulsar content of archival data from the SMC. This monitoring has revealed eight previously undiscovered X-ray pulsars (Macomb et al. 1999, Finger et al. 2001, Lamb et al. 2002a, Lamb et al. 2002b, Macomb et al 2003). In addition, analysis of XMM-Newton data for the possible Anomalous X-ray Pulsar (AXP), CXOU J010043.1-721134, (Lamb et al. 2002b, 2003) clearly establishes its pulse period to be 8.02 s, with characteristics which support its likely identity as an AXP.

In the following section we present the X-ray observations and analysis relating to the two newly discovered X-ray pulsars and the possible AXP. Section three deals with the optical identification of the 202 and 263 s pulsars with high mass objects in the SMC. Each of the three pulsars are then briefly discussed in Section 4.

Finally in Section 5, we present an overview of the SMC HMXB pulsars. In particular we note that virtually all of the SMC HMXBs are located in young (ages $\leq 3 \times 10^7$ years) star forming regions as expected on the basis of binary evolution models (Verbunt & van den Heuvel 1995). We note a significant inverse correlation between period and maximum X-ray flux density for those HMXBs with Be companions. This correlation may be a reflection of the fact that for such objects spin period is correlated with orbital period (Corbet 1986) and longer period Be HMXBs have lower maximum accretion rates. We note a similar correlation between X-ray luminosity and spin period for the Be HMXB pulsars of the Milky Way. We find no significant difference between the distribution of periods from the HMXBs of the SMC compared with that of the Milky Way, except

for a slight deficit for SMC pulsars with periods longer than \sim 200s. This may be due to their generally smaller luminosity compared to the luminosity of SMC HMXB pulsars with faster spin.

2. X-ray Observations

Table 1 gives a list of the XMM-Newton archival data which were surveyed for this paper. Data from the European Photon Imaging Cameras EPIC PN (Strüder et al. 2001), and M1 and M2 (Turner et al. 2001) were utilized. For the first stage of the analysis, we utilized the data products of the Pipeline Processing Subsystem (PPS files) to search for pulsars. Point-like sources were identified from image files and circular selection regions around each source were chosen by eye. Radii of selection circles varied from 15 to 32.5 arc seconds depending on source strength and position in the field of view. Sources with fewer than \sim 500 photons were not examined. With this cut-off a total of 63 sources were selected for timing analysis.

Two previously undiscovered pulsars were detected by this analysis and the period of the possible AXP reported by us (Lamb et al. 2002, 2003) was correctly determined. Timing and spectra for each of these sources is presented below.

The selection circles for each source provide a spatial filter to make photon event lists from the PPS event files. Photon arrival time information was then used in a search for significant periodicities at frequencies less than the Nyquist limit of each dataset. This limit depends on the data mode of each instrument. Generally for PN data, the Nyquist limit was 6.8 Hz, for the MOS data, the limit was generally 0.19 Hz. Initial Fourier transforms were performed separately on the two data types, PN and MOS.

In the first pass through the data no significant frequency greater than 0.19 Hz was detected. To increase the sensitivity to a possible signal, data from all three detectors (M1, M2, and PN if available) were merged for further analysis. With this combined data, three different energy selections were made: all energies, energies above 1 keV, and energies above 2 keV. With this procedure two significant periodicities were discovered, 202 s and 263 s, the details of which follow. In addition to these periodicities, seven previously known pulsars were also detected: pulsars with periods of 172, 323, and 755 s in the field of observation 0110000101, pulsars with periods of 152, 280, and 452 s in the field of 0110000201, and the possible AXP, CXOU J010043.1-721134, with a pulse period of 8.02 s rather than the previously reported 5.4 s (Lamb et al. 2002b).

The event selection for our spectroscopic studies of these three sources utilized the XMM-Newton Science Analysis System (SAS) (version 5.3) software from the XMM-Newton Science Operations Center (SOC). The data were filtered to remove “bad” pixels and events falling at the edges of the CCDs. We retained only standard XMM-Newton event grades (patterns 0-12 for MOS1 and MOS2, and patterns 0-4 for the PN instrument).

A spectrum was extracted, using the *evselect* program in SAS, grouping photons to the nominal

detector energy resolution of 15 eV for the MOS instruments and 5 eV for the PN instrument. An energy cut was applied to include only events in the energy range 0.25-10.0 keV. For estimating the background, we chose several source free regions in the same CCD as our target source. The results of the spectral analysis were not sensitive to the choice of the background region chosen. All spectral fits employed the XSPEC v11.2 software fitting package.

2.1. 1XMMU J004723.7-731228. 263 s Pulsar

This pulsar was discovered in the analysis of observation 0110000101, a field rich in X-ray pulsars. Recently Haberl & Pietsch (2004) reported detection of 263 s pulsations from this same source. Thirteen sources in observation 0110000101 meet the criterion of a minimum of 500 photons, including three previously detected as pulsars. Our analysis detected pulsations from all three.

The initial selection circle for J004723.7-731228 was 25 arc seconds. Significant power was separately detected at a fundamental frequency of 0.0038 Hz for both the M1 and M2 combined data (normalized power 28) and PN data (normalized power of 29). These Fourier power values are consistent with the near equality of the number of selected photons for the two different types of detector. In the Fourier analysis of the combined dataset (PN plus MOS) a normalized power of 56 was obtained with evidence for significant power for the next three higher harmonics.

In order to maximize our sensitivity to the pulsed signal two optimization procedures were further employed. By using the strength of the Fourier power at the fundamental plus the next four harmonics as a criterion, a search on position and radius of a selection circle was performed. A search was also made to establish the optimum energy selection. After these two optimizations, a normalized Fourier power (fundamental) of 81 resulted, with a power of 150 for the sum of the first five harmonics. The optimum selection circle for the PN data was 27.5 arc seconds, for the MOS data 32.5 arc seconds. The optimum energy selection required the photon energy to be between 0.1 keV and 5.0 keV.

Figure 1 (a) shows the resulting optimized Fourier transform for J004723.7-731228. The fundamental, barycentered frequency is 0.003803 (3) Hz, with significant power clearly visible at the second, third and fourth harmonics. This frequency corresponds to the pulse period of 263.0 ± 0.2 s. The pulse profile is shown in Figure 1 (b). The dashed line indicates the non-source background level. The pulsed fraction is $47 \pm 4\%$. The epoch of the observation is 51832.684 MJD.

In the case of the 263s pulsar (1XMM J004723.7-731228), this source was detected at coordinates R.A. = $00^h 47^m 23.7^s$, Dec. = $-73^\circ 12' 27.7''$ (J2000). A selection circle of radius $30''$ was used, resulting in 7931 photons (2736 photons in MOS1, 1817 photons in MOS2, and 3378 photons in PN). The background is estimated to be 252 photons.

In addition, for the 263s pulsar, we produced a pulse-resolved spectrum. The SAS *barycen* program was used to transform the times of arrival of the photons for this source, using the best

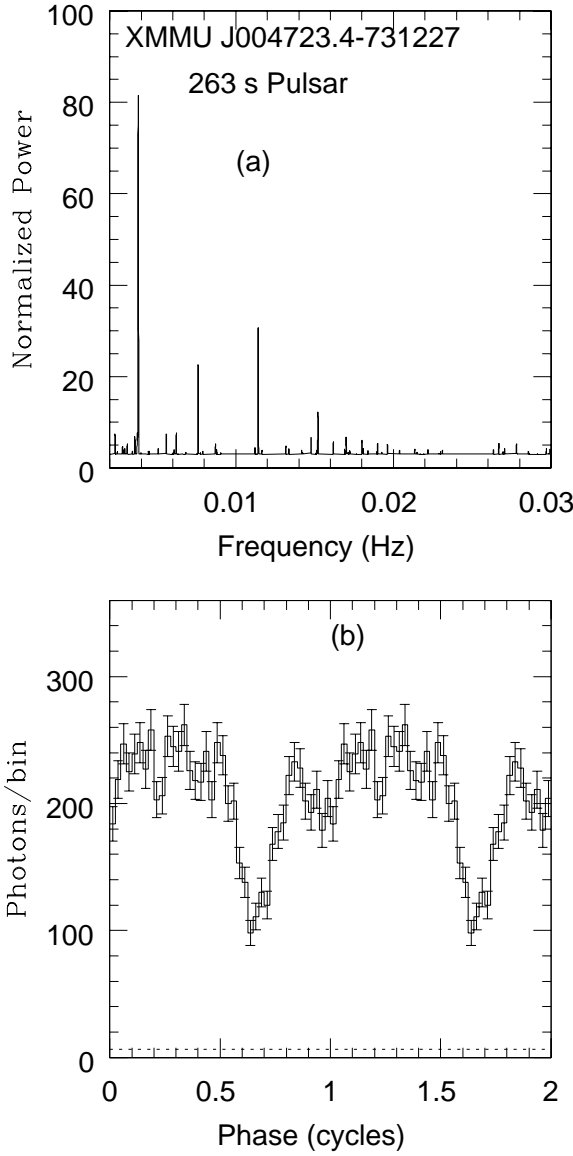


Fig. 1.— (a) A portion of the FFT for 1XMMU J004723.7-731228. In addition to power at the fundamental frequency of 0.003803(3) Hz, there are clear power peaks at the second, third, and fourth harmonics. (b) Pulse Profile of 1XMMU J004723.7-731228. The dashed line indicates the non-source background level.

period obtained from our timing analysis, to the solar system barycenter. After extracting the spectra, to ensure sufficient S/N for subsequent fitting, we re-bin them to ensure a minimum of 30 counts per energy bin for the 202s pulsar and 20 counts per bin for the 263s pulsar. With this set of choices for the minimum count per bin, it appears that we are not losing any features in the spectra. The net count rate after the sequence of filters described for each source in each instrument is given in Table 2.

The spectral data from the three EPIC instruments were fitted simultaneously. We attempted to fit the spectra to various models. In each trial, all model parameters were allowed to vary freely, but were constrained to maintain the same value for each spectra. To account for the slightly different count rates in each detector, an overall normalization parameter is allowed to vary for each data set. The spectrum is best fit with a composite model consisting of power-law and blackbody components, modified by neutral absorption. (see Figure 4). With this model we obtain an acceptable $\chi^2/\nu = 1.02$ for 278 degrees of freedom. Best fit parameter values for this model are listed in Table 2.

2.1.1. Pulse Profile for Different Energy Bins

Using the best period and combining the data from the three instruments, we calculated a phase for each event passing our event selection criterion. The pulse profile can be characterized as a broad peak, with one or possibly two dips within this overlying envelope.

To search for any energy dependent features in the folded light curve, four contiguous energy intervals were chosen: I: 0.3-1.0 keV, II: 1.0-2.5 keV, III: 2.5-5.0 keV, IV: 5.0-10.0 keV (see Figure 5). We can identify the first dip in the broader pulse profile in all but the last energy interval (IV). We note that there is a marginal feature near the second dip in the 0.3-1.0 keV interval, which could simply be due to statistical fluctuations.

2.1.2. Phase-Resolved Spectra

To search for possible spectral variation as a function of the pulsar rotation phase, we divided the data into five phase intervals. The phase intervals correspond to the first pulse-on ($\phi = [0.0 - 0.48]$), first pulse-off ($\phi = [0.54 - 0.71]$), second short pulse-on ($\phi = [0.76 - 0.86]$), and the second pulse-off interval ($\phi = [0.88 - 0.99]$). We subsequently divided the first pulse-on interval into two contiguous ones, to assure that we have comparable statistics in each phase interval. Doing so also served as a consistency check of our fitting procedure, which should give comparable results for the two intervals.

The spectrum for each phase interval was then fitted to the optimal power-law plus blackbody model obtained for the overall spectrum. We only allowed the overall normalizations to vary, fixing

Table 1. Observations of the SMC by XMM-Newton searched for X-ray pulsars

Obsid ID	RA (J2000)	DEC (J2000)	Duration(ks)	Comments
0018540101	00 59 26.8	-72 09 55	27.3	8.0 s Possible AXP
0084200101	00 56 41.7	-72 20 24	21.5	
0084200801	00 54 31.7	-73 40 56	21.9	
0110000101	00 49 07.0	-73 14 06	29.5	263 s Pulsar
0110000201	00 59 26.0	-72 10 11	21.2	202 s Pulsar
0110000301	00 54 52.0	-72 23 10	36.3	
0135720601	01 03 43.5	-72 01 55	30.3	
0135720801	01 04 00.0	-72 00 16	33.3	
0135720901	01 04 01.7	-72 01 51	36.0	
0135721001	01 04 01.7	-72 01 51	32.4	
0135721301	01 03 56.4	-72 00 28	28.9	
0011450101	01 17 05.1	-73 26 35	59.8	SMC X-1 region
0011450201	01 17 05.1	-73 26 35	41.3	SMC X-1 region

Table 2. Spectral Parameters of Reported Pulsars.

Source	$\chi^2/(dof)$ (dof)	kT(keV)	$N_{bb}(10^{-5})$	α	$N_{pl}(10^{-4})$	n_H	L_x (ergs/s)
J004723.7-731228	1.02(278)	2.2(1)	4.6(5)	1.7(3)	2.2(2)	3.4(5)	1.1×10^{36}
J005920.8-722316	0.99(20)	-	-	1.10(16)	0.80(36)	0.9(8)	3.4×10^{35}
J010043.1-721134	0.92(30)	-	-	2.85(8)	3.6(4)	0.30(2)	2.4×10^{35}

Note. — The normalization (N) of either the power-law or the blackbody spectrum have units of $cm^{-2}s^{-1}$. Units of $n_H \times 10^{21} cm^{-2}$. The luminosity is for the energy interval 0.2-6 keV.

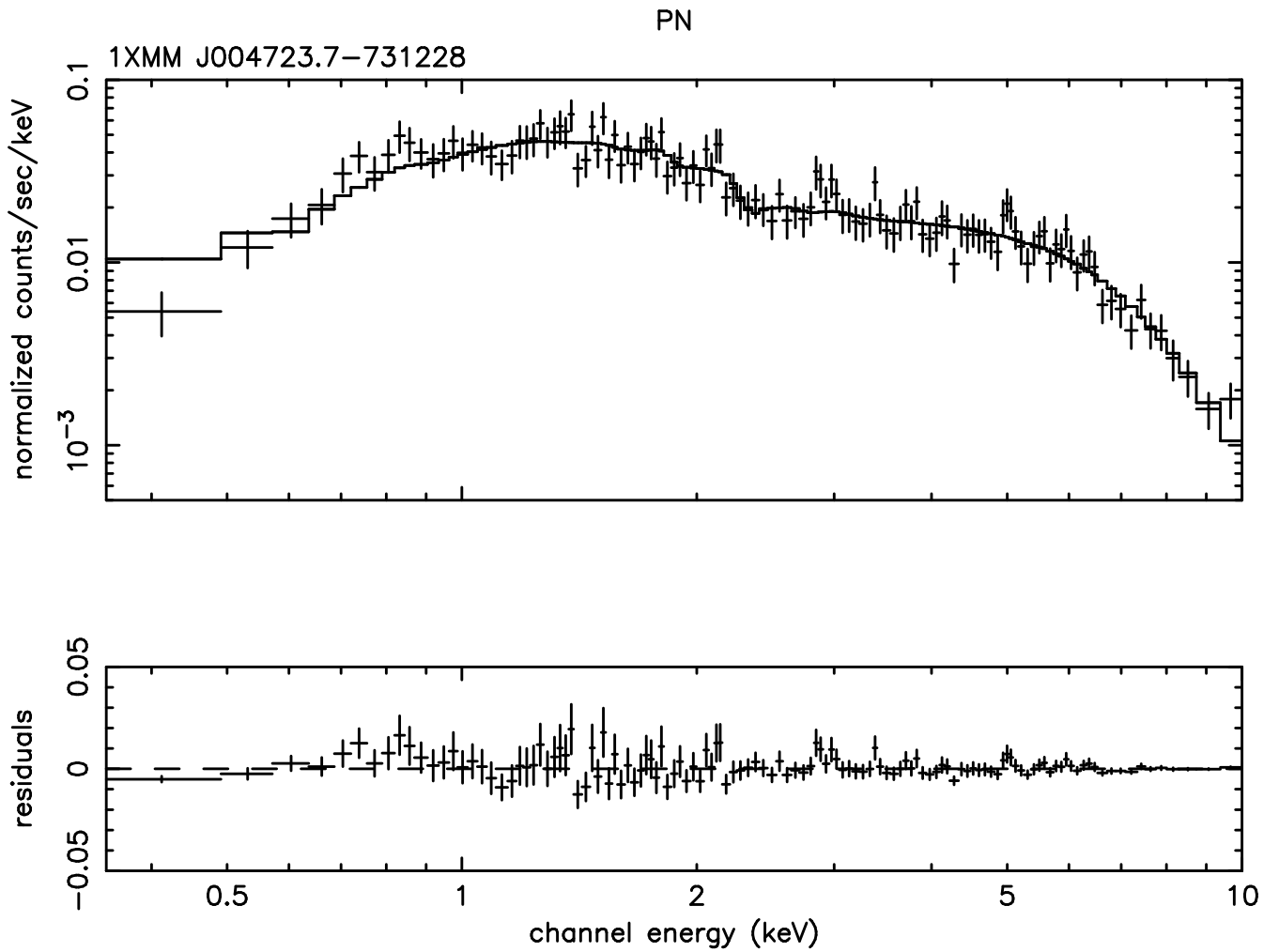


Fig. 4.— Spectrum of 1XMMU J004723.4-731227. The fit shown is a composite model for the PN detector consisting of power-law and blackbody components, modified by neutral absorption. Parameter values are given in Table 3.

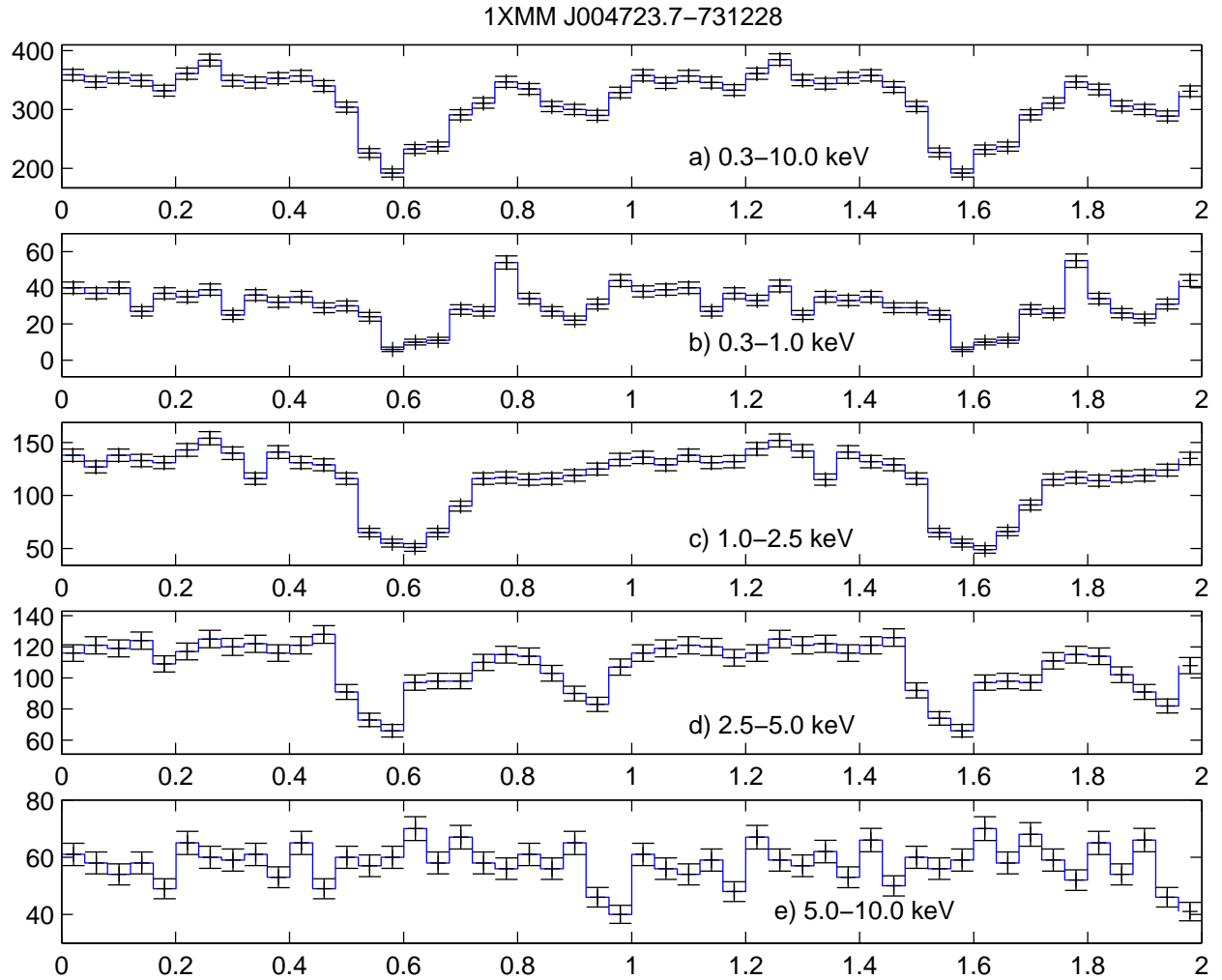


Fig. 5.— Pulse profile for 1XMMU J004723.7-731228 for various energy selections. (a) 0.3-10. keV. (b) 0.3-1.0 keV. (c) 1.0-2.5 keV. (d) 2.5-5.0 keV. (e) 5.0-10.0 keV.

the other fit parameters to their nominal values from the overall fit. The results of the fitting procedure is shown in Table 3.

Our results suggest that the best fit model obtained in the overall fit is an acceptable model for the first pulse-on and the second dip intervals. The results for the second dip is marginal, given the limited statistics. However, the spectrum during the first pulse-off region is clearly not well described by this model. There is a slight deficit of events in the lower energy region and a clear excess of events in the higher energy bins above 5 keV.

Despite the limited statistics, we attempted to model the spectrum during the first pulse-off region. Both a simple blackbody model as well as a simple power-law model (modified by neutral absorption in the ISM) results in acceptable fits. From the blackbody model, we obtained a temperature of $kT = (2.3 \pm 0.2)\text{keV}$, with a reduced χ^2 of 1.09 (null probability of 0.32). The simple power-law model resulted in an $\alpha = 0.25 \pm 0.1$, $n_H = (0.4 \pm 0.2) \times 10^{22}\text{cm}^2$, with a reduced χ^2 of 1.14 (null probability of 0.25).

2.2. 1XMMU J005920.8-722316. 202 s Pulsar

This pulsar was discovered in an analysis of observation 0110000201, a field even richer than observation 0110000101 in the proportion of sources which have been established as binary X-ray pulsars. Of the seven sources in this field which have more than 500 photons, 4 have been previously reported to be X-ray pulsars. Our timing analysis detected 3 of these previously known pulsars, only the possible AXP, CXOU J010043.1-721134 (Lamb et al. 2002b) was not detected. (However clear pulsations from this latter source were detected from another observation, 0018540101, and this detection is discussed in a subsection below.) The position of the 202 s pulsar (1XMM J005920.8-722316) is: R.A. = $00^h 59^m 21.05^s$, Dec. = $-72^\circ 23' 17.1''$ (J2000).

For 1XMMU J005920.8-722316, no significant Fourier power was detected in either the uncut data, nor the data selected to have photon energies greater than or equal to 1.0 keV. However, for photons with energies greater than 2.0 keV, highly significant power of 26.6 (chance probability, after consideration of the frequency and energy search ranges of less than 6×10^{-7}). Optimization

<i>PhaseInterval</i>	χ^2/dof (dof)	<i>NullProbability</i>	<i>Flux</i> [$\times 10^{-13}\text{ergs cm}^2\text{s}^{-1}$]
0.00-0.28	0.96 (104)	0.58	8.75
0.28-0.48	1.02 (78)	0.43	6.54
0.54-0.71	3.13 (42)	$< 10^{-10}$	3.38
0.76-0.86	1.41 (33)	0.06	3.02
0.88-0.99	0.72 (34)	0.89	3.00

Table 3: Phase Dependent Spectral Fit Results for 1XMMU J004723.7-731228.

of the region and energy selected gave a final power of 30 at 0.004954 (12) Hz, with a final energy cut of 1.9 keV and a circle of selection of 27.5 arc seconds. There is small, but significant power (4) at the second harmonic. The frequency of the fundamental corresponds to a pulse period of 201.9 ± 0.5 s. Figure 2 (a) shows a portion of the resulting Fourier transform for this source. Figure 2 (b) shows the pulse profile at this frequency. The pulsed fraction is: $50 \pm 8\%$. The epoch of the observation is 51834.633 MJD.

This source also present in observation 008420001, 528.9 days later than observation 0110000201. In this observation the source flux is 70% of that of the earlier observation. A Fourier transform of the source photons with a similar energy selection as that done for 0110000201 reveals a power of 15 at a frequency of 0.004968 (12) Hz (201.2 ± 0.5 s pulse period). Although this is not a highly significant detection, we regard it as supporting evidence for the 202 s pulsation. The difference in frequency between the two observations is $14 \pm 17 \mu\text{Hz}$ which is not significant. A upper limit on a frequency derivative over the interval between the two observation is $3 \times 10^{-13} \text{ Hz/s}$.

The spectral data from the two MOS instruments were fitted simultaneously. The spectrum is best fit with a simple power-law model, modified by neutral absorption. Each model parameter is allowed to vary freely, but was constrained to maintain the same value for both spectra. An overall normalization parameter for each data set is allowed to vary to account for the slightly different count rates in each detector. With this model we obtain an acceptable $\chi^2/\nu = 0.996$ for 20 degrees of freedom. Best fit parameter values for this model are listed in Table 2. As a consistency check, we attempted to fit each spectrum with a power-law model, fixing the value for n_H to the optimal value obtained in the combined fit. The resulting fits give acceptable χ^2 with values for the parameter α consistent with the results of the combined fit.

We also attempted to fit a model consisting of power-law and blackbody components, modified by neutral absorption. We obtained a somewhat higher, yet still adequate, $\chi^2/\nu = 1.10$ for 18 degrees of freedom. However, the blackbody temperature obtained is unreasonably high and is not constrained by this fit ($3 \pm 60 \text{ keV}$). We note that a simple blackbody model results in a very poor fit ($\chi^2/\nu = 3.6$ for 18 dof).

2.3. Possible AXP, CXOU J010043.1-721134

This source was first reported as a 5.4 s (frequency 0.184 Hz) pulsar by Lamb et al. (2002b) from an analysis of *Chandra* ACIS-I data. In the Fourier transform of the *Chandra* data two power peaks appeared, one at 0.125 Hz just below the ACIS-I Nyquist frequency, and the other at 0.184 Hz. The two peaks are aliases of each other. Our efforts to remove this frequency ambiguity used ROSAT observations and concluded (erroneously) that the correct frequency was 0.184 Hz. Our present analysis of XMM data using PN data from observation 0018540101 decisively settles the question of the pulse period. The PN data has a Nyquist frequency of 6.8 Hz, far above the region of interest.

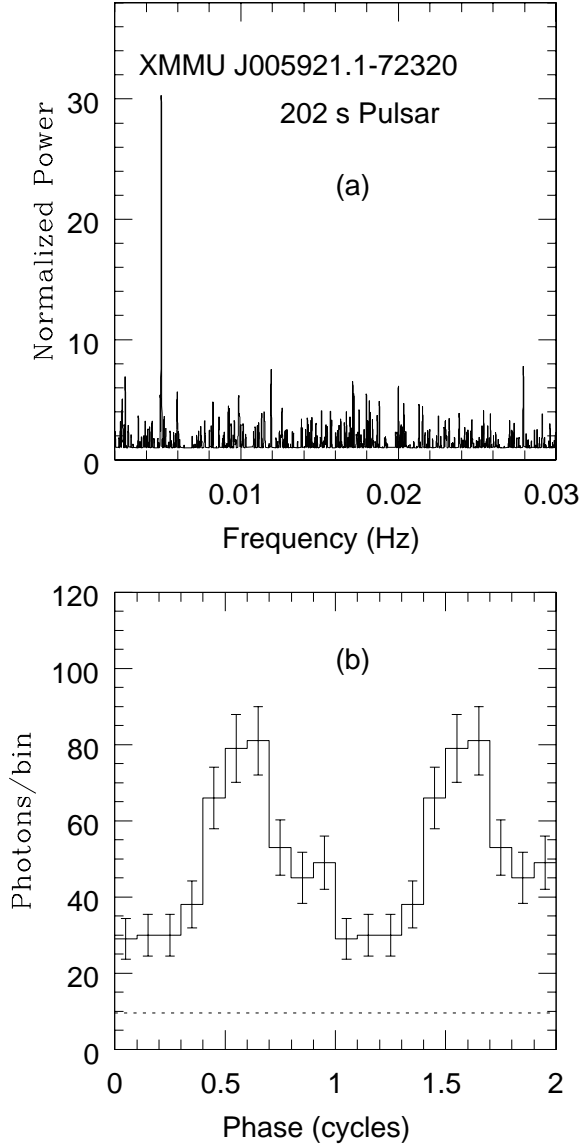


Fig. 2.— (a) A portion of the Fourier transform for 1XMMU J005921.1-722320. The peak frequency is 0.004954 (12) Hz corresponding to a period of 201.9 s. (b) Pulse Profile of 1XMMU J005921.1-723020. The dashed line indicates the non-source background level.

A selection circle 30 arc seconds in radius around the source region produced 4048 photons. The times of arrival for these photons were corrected to the barycenter of the solar system using the SAS software. The Fourier transform of these corrected times showed a strong, normalized power 28, peak at a frequency of 0.124699(5) Hz. A selection of photons with energies less than 6.0 keV increased this power to more than 30. The FFT of these energy selected photons is shown in Figure 3 (a). In addition to the peak at the fundamental there is a clear signal at the second harmonic as well as a much weaker signal (power 11) at the third harmonic. The pulse profile for these photons at this frequency is shown in Figure 3 (b). The pulsed fraction is $33\pm5\%$.

The epoch for this observation is 52234.015 MJD. The initial *Chandra* observation (Lamb et al. 2002b) occurred 189.934 days earlier and the observed frequency for that epoch was 0.124706(1) Hz. By combining the two observations we derive a frequency time derivative of $-4\pm3 \times 10^{-13}$ Hz/s. This corresponds to a characteristic timescale, P/\dot{P} , of ~ 10 kyr, consistent with the similar timescales observed for other AXPs (See Mereghetti et al. 2002 for a review).

The spectrum for this source was fitted to the PN data of observation 0018540101. The spectrum of the source is well fit with a simple power-law or a combination of power-law and blackbody components. However, the fit using the combination of power-law and blackbody did not constrain the normalization of either component, with the size of the errors on each normalization comparable to the value of the normalizations. Figure 6 shows the best fit to the data using the simple power-law model, modified by neutral absorption. The best fit parameters are given the Table 4.

3. Observations at Other Wavelength

Further understanding of the 202 and 263 s pulsars requires identifying their optical counterparts. To this end, we have searched for stars at other wavelengths that are within a distance from the XMM centroid location of 1.5 arcseconds plus the position error of the putative counterpart. The X-ray component of this radius is slightly beyond the typical systematic error on XMM positions of 1.3 arcseconds as given in the XMM-Newton User’s Handbook. Table 3 lists catalog information of the best candidate for each pulsar from two different star catalogs. For both pulsars, the two optical counterparts listed are consistent with being the same source. The star catalogs used are the OGLE SMC catalog (OGLE; Udalski et al. 1998) and the Magellanic Clouds Photometric Survey (MCPS; Zaritsky et al. 2002.)

For the 263 second pulsar, there are stars in both the OGLE and MCPS catalogs which are 0.91 and 1.29 arcseconds away from the putative XMM position. The OGLE survey has a typical source localization of 0.15 arcseconds with a possible systematic error as large as 0.7 arcseconds. For the MCPS catalog, the distributions of angular offsets peak at $0.3''$ and most stars are localized to within 1.0 arcseconds. The angular distance between these two catalog stars is only 0.4 arcseconds, consistent with being the same source. As Table 3 shows, the measured magnitudes of both stars are

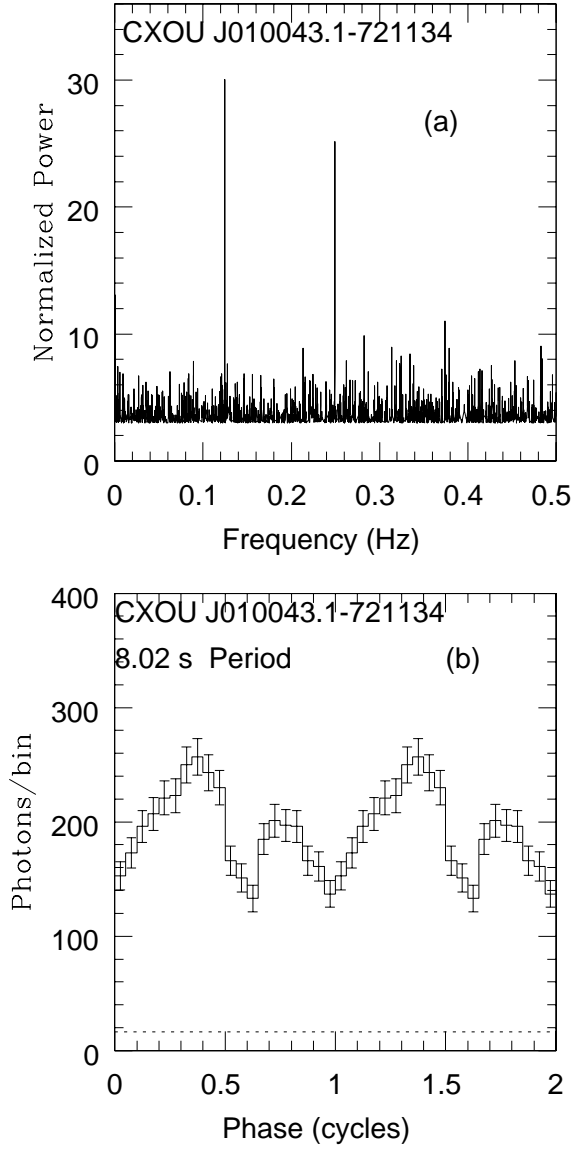


Fig. 3.— (a) A portion of the Fourier transform for CXOU J010043.1-721134 (1XMMU J010043.1-721134). The peak at 0.1248 Hz corresponds to the fundamental frequency of the possible AXP. Also second and third harmonics are visible as well. the (b) Pulse Profile of CXOU J010043.1-721134. The dashed line indicates the non-source background level.

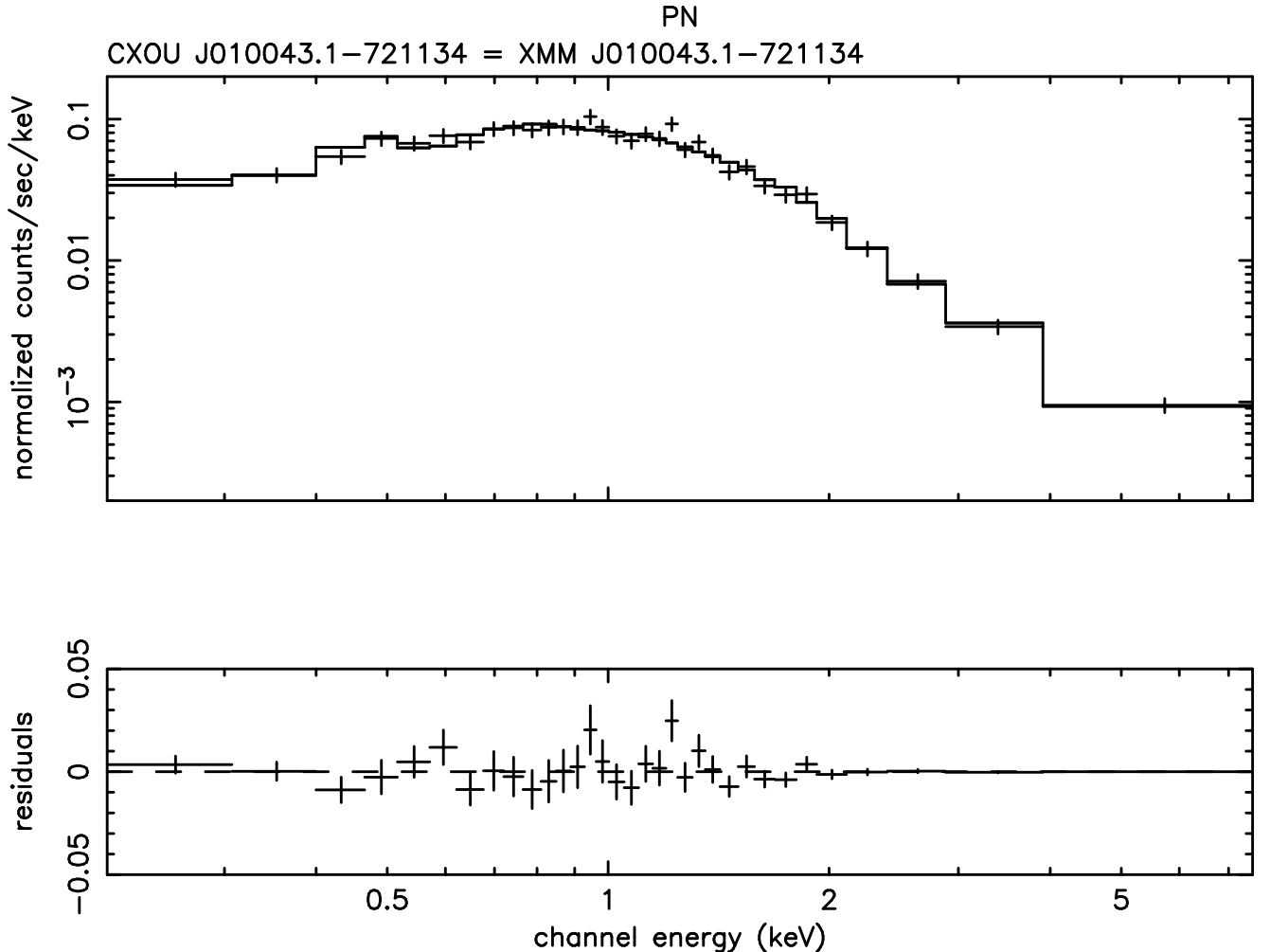


Fig. 6.— Best fit spectrum for CXOU J010043.1-721134 for a model with a power-law modified by neutral absorption. The parameters for this model are given in Table 4.

Table 4. Proposed Optical Counterparts to the Two Newly Discovered Pulsars

Source	Catalog	Cat. Num.	R.A.	Dec.	Dist.(“)	M_B	B-V
1XMM J004723.7-731228	MCPS	1713720	00 47 23.42	-73 12 27.3	0.91	16.11(2)	-0.08
	OGLE	114733	00 47 23.35	-73 12 27.0	1.29	16.10(1)	-0.04
1XMM J005920.8-722316	MCPS	3345630	00 59 21.04	-72 23 16.7	0.11	14.96(2)	-0.11
	OGLE	151891	00 59 20.69	-72 23 17.0	0.37	14.76(2)	-0.07

consistent. The B magnitude (-2.8), color index of this star, (B-V = -0.08), and a distance modulus for the SMC of 18.9 (Dolphin et al. 2001)) are consistent with a B2 star (Allen’s Astrophysical Quantities 2000).

The 202 second pulsar is similar, with stars in both the MPCS and OGLE surveys being consistent in position with the XMM position and with each other (0.3 arcseconds apart). This tentative counterpart is somewhat brighter with a B magnitude of -4.1 approximately consistent with a B0 star. In both cases, the B-V value is roughly that expected with the expected given the galactic reddening (Hill et al. 1994).

4. Discussion

4.1. Possible AXP–CXOU J010043.1-721134

If the possible AXP is located in the SMC at a distance of 60 kpc, its luminosity is 2.4×10^{35} ergs/s. This luminosity is well within the range of luminosities given for AXPs (see for example Mereghetti et al. 2002). This luminosity is $\sim 50\%$ larger than the average luminosity given for this source in the compilation of luminosities given by Lamb et al. 2002b. Given that this luminosity is obtained with a different instrument than those of given in Lamb et al., we do not regard this feature as disqualifying the candidacy of the source as an AXP which generally have near constant luminosity. The observed spin-down time scale of the source, P/\dot{P} , of ~ 10 kyr is similar to the values obtained for other AXPs which are in the range of $10^{4-5.5}$ yr. By establishing the correct period to be 8.02 s rather than 5.4 s we remove what would have been the shortest period AXP and replace it with a candidate AXP whose period is nearly equal to the average of the 6 AXPs given in Mereghetti et al.(2002).

4.2. Two Newly Discovered X-ray Pulsars

We have described the discovery of two high-mass X-ray binary systems in the Small Magellanic Cloud. Both pulsars are somewhat typical for their class - having hard spectra and identified with early B stars. They differ in that they are in the upper third of the distribution of pulse periods for SMC high-mass X-ray binaries and in that there is currently no evidence that they are associated with an emission line source as the counterpart. A much larger percentage of SMC pulsars are in the Be category as compared to the Milky Way (Haberl & Sasaki 2000). These two pulsars do not seem to be associated with supergiant stars but neither have they been reported as emission line sources.

5. The High Mass X-ray Binary Pulsars of the SMC

In Table 5 we list all of the HMXB pulsars of the SMC which have been optically identified. The list is compiled from the HMXB list of Liu et al. (2000) with additional pulsars from ASCA observations summarized by Yokagawa et al. (2003), an additional pulsar from XMM-Newton observations by Sasaki et al. (2003) plus the two newly discovered pulsars discussed in this paper. In addition, in Table 6 we list all other X-ray pulsars of the SMC of which we are aware. Some of these may in fact be HMXBs but they lack an optical identification.

In Figure 7 we have plotted the locations of the pulsars of Table 5 and 6 overlaid on contours of recent star formation in the SMC taken from Figure 7 of Maragoudaki et al. (2001). The contours show the density of young stars having ages $(1.2 - 3) \times 10^7$ yr. (Note: Our Figure 7 is similar to Figure 12 of Yokogawa et al. (2003), however, we have chosen to plot only established pulsars rather than including candidate HMXBs as Yokogawa et al. do.) In view of the formation history of HMXBs (Verbunt & van den Heuvel 1995) the correspondence between the young stars and HMXBs is to be expected. If there were significant discrepancies between the spatial locations of the HMXBs and regions of young stars, then our understanding of the evolution of X-ray binaries would need modification. A conclusion to be drawn from this figure is that most of the X-ray pulsars of Table 6 not yet identified as HMXB pulsars may be high mass binaries.

The overabundance of the SMC HMXB pulsar population relative to that of the Milky Way has been noted many times before (cf Yokogawa et al. 2003). For example in the compilation of HMXBs of Liu et al. (2000) there are 50 HMXB pulsars listed for the Milky Way whereas for the SMC with approximately 1% of the mass of the Milky Way we have compiled a list of 24 HMXB pulsars (Table 5). There are absorption and sky coverage effects that may diminish the number of detected HMXBs for the Milky Way, nevertheless, on the face of it the SMC population of HMXBs is overabundant relative to the Milky Way by a factor of ~ 50 . This points to a spectacular episode of star formation in the SMC beginning approximately 30 million years ago.

One of the advantages of population studies with the SMC is its well known distance. Thus fluxes are proportional to luminosity, a fundamental parameter of each binary system. We have investigated the possibility of a correlation between the spin period of the neutron star and its luminosity using the maximum reported flux density. We have restricted this investigation to the subset of the HMXBs in Table 5 which are firmly identified with Be companions. On the basis of a simple model of the accretion process for such objects, discussed below, one might expect that rapid rotation leads to greater maximum luminosity. We find empirically that notion is supported by the observations.

In Figure 8(a) we have plotted the maximum X-ray flux density versus spin period for the Be HMXBs. (Note: we have added four Be HMXB pulsars from the LMC and scaled their flux densities to the distance of the SMC; 64 kpc for the SMC, 55 kpc for the LMC. The LMC sources are: 0535-668, J0544.1-7100, J0502.9-6626 and J0529.8-6556.) The maximum flux densities are anti-correlated with spin periods, having a correlation coefficient of -0.75. The probability that

Table 5. High Mass X-ray Binaries in the SMC

Source	Period (s)	Type	Flux Density) ^x	References
0115-737 (SMC X-1)	0.71			a
SMC X-2	2.37	Be	7.6	b
J0059.2-7138	2.76	Be	18	a,b
J0051.8-7231	8.90	Be	0.34	a,b
J0052.1-7319	15.3	Be	12.3	a,b
J0117.6-7330	22.1	Be	9.2	a,b
J0111.2-7317	31.0	Be	16	a,b
J0053.8-7226	46.6	Be	0.15	a,b
RX J0054.9-7226	59.0	Be	0.76	b
J0049-729	74.7	Be	0.49	a,b
J0051-722	91.1	Be	3.0	a,b
XMMU J005605.2-722200	140.			c
CXOU J005750.3-720756	152.			d
J0054-720	169.	Be	4.3	a,b
AX J0051.6-7311	172.	Be	0.19	b
1XMMU J005920.8-722316	202.			e
1XMMU J004723.7-731228	263.			e
J0058-7203	280.			a,b
CXOU J010102.7-720658	304.			d
J0050.7-7316	323.	Be	0.19	a,b
1SAX J0103.2-7209	349.	Be	0.14	b
RX J0101.3-7211	455.	Be	0.28	b
CXOU J005736.2-721934	565.			d
AX J0049.5-7323	756.			b

^xMaximum X-ray flux density in units of μJy . $1 \mu\text{Jy} = 2.4 \times 10^{-12} \text{ ergs/s/cm}^2/\text{keV}$.

Note. — The maximum X-ray flux density is calculated from flux values cited in the original papers given in the references. We approximate the flux density as flux divided the energy interval over which the flux is measured, generally 0.1 to 2.5 keV (ROSAT) or 2.0 to 10. keV (ASCA and Chandra). This approximation is valid if the source spectrum has a power-law dependence with number index -1. References: a=Liu et al. (2000), b=Yokagawa et al. (2003), c=Sasaki et al. (2003), d=Macomb et al. (2003), e=This work

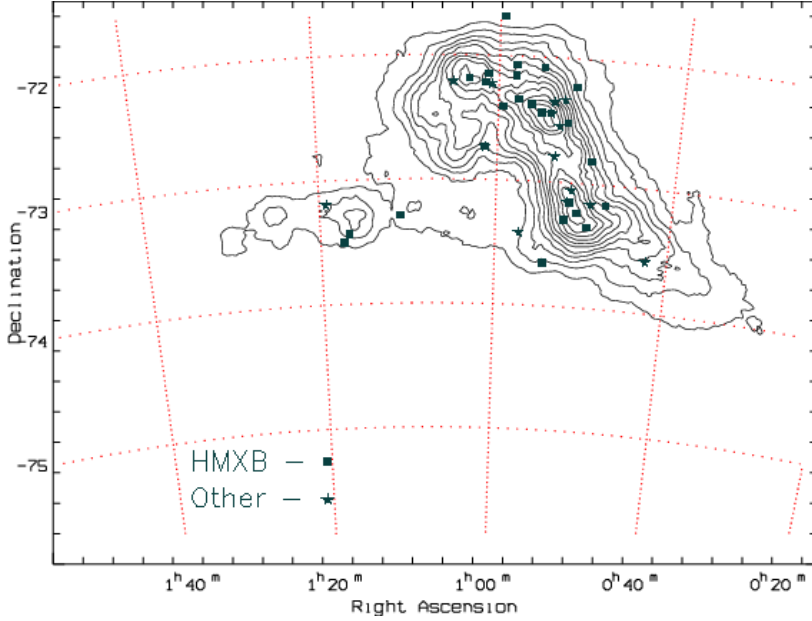


Fig. 7.— Locations of the HMXBs of the SMC relative to its young star forming regions. The contours are those of Figure 7 of Maragoudaki et al. (2001), corresponding to contours of constant star density for stars with ages $(1.2 - 3) \times 10^7$ yr. Note that XTE positions (nine of the stars) are uncertain by as much as a degree.

Table 6. Other X-ray Pulsars in the SMC

Source	Period (s)	References
AX J0043-737	0.0876	Yokogawa & Koyama (2000)
XTE J0119-731	2.17	Corbet et al. (2003a)
AX J0105-722	3.34	Yokogawa & Koyama (1998)
XTE J0052-723	4.78	Corbet et al. (2001)
XTE J0103-728	6.85	Corbet et al. (2003b)
XTE Position A	7.77	Corbet et al. (2003c)
CXOU J010043.1-721134	8.02	Lamb et al. (2002b, 2003)
AX J0049-732	9.13	Imanishi et al. (1998)
XTEJ0050-732#1	16.6	Lamb et al. (2002a)
XTEJ0050-732#2	25.5	Lamb et al. (2002a)
XTE J0052-725	82.4	Corbet et al. (2002)
XTE SMC95	95.0	Laycock et al. (2002)
AX J0057.4-7325	101.	Yokogawa et al. (2000)
XTE J0103-728	144.	Corbet et al. (2003b)

there is no correlation between spin period and maximum flux density is 2×10^{-4} . The solid line in Figure 8(a), a least square fit to the points, has a slope of -0.73 ± 0.16 .

A similar correlation is found for the Be HMXB pulsars of the Milky Way. Haberl & Sasaki (2000) list the spin period and maximum luminosity of 27 HMXB pulsars of the Milky Way (their Table 3). We have plotted these data in Figure 8(b). The data are strongly correlated, correlation coefficient of -0.69 , with a probability of 6×10^{-5} that the correlation is by chance, and a fitted slope of -1.01 ± 0.21 . We have combined the data for the Milky Way and for the Magellanic clouds into a single plot, shown in Figure 9. We have scaled the Magellanic cloud data to an SMC distance of 60 kpc. The correlation coefficient for this combined data, Milky Way plus the Magellanic Clouds (46 points), is -0.71 with a probability that it is due to chance of 2.9×10^{-8} . The fitted slope has a value of -0.95 ± 0.14 .

Many HMXBs are transients with large variation in flux. This fact undoubtedly contributes to the scatter of the points of Figure 8 and 9. Nevertheless there is a significant inverse correlation between maximum X-ray flux density and period. This correlation should be understandable in terms of the physics of the accretion process. In a simple model of accretion from the stellar wind of the Be companion, the rate of accretion onto the neutron star is proportional to the density of the wind, which depends on $1/r^n$ where r is the distance between the companion and the neutron star. “n” is found to range from 2 to 4, but mostly between 2.5 and 3 (Waters & van Kerkwijk 1989). We take $n=3$. By Kepler’s law, r goes as $P_{orb}^{2/3}$ of the neutron star. Empirically spin period for Be HMXBs is proportional to P_{orb}^2 (Corbet 1986). Thus luminosity should scale roughly as P_{spin}^{-1} , implying a slope of -1 for the correlation of the data points of Figures 8 and 9 in rough agreement with what is observed. Note that only four of the Be systems listed in Table 5 have measured orbital periods. P_{spin} , because of the Corbet relation, thus becomes a surrogate for P_{orb} .

Of course there are many complications to this very simple analysis. One complication is that, for highly elliptic orbits, mass transfer from the companion to the neutron star will occur near periastron and thus the appropriate scaling distance is significantly less than r . Nevertheless, further work on this demonstrable correlation between spin period and X-ray luminosity may be fruitful. It could be that a suitably improved relation would serve as a distance indicator. We have found that the maximum degree of correlation between the Magellanic Clouds and the Milky Way is achieved if the luminosities are reduced by roughly $2/3$ of their value, which would imply a distance reduced by $\sim 18\%$. Since we believe that the distances to the LMC and the SMC are rather well determined a more likely possibility is that the Magellanic Be HMXBs are perhaps more luminous than those of the Milky Way. Another possibility is that the estimates of the distances of the Milky Way sources are inaccurate, and their luminosities in general need to be increased.

We have compared the period distribution of SMC population of HMXB pulsars to that of the Milky Way. In Figure 10, the cumulative distributions of pulse periods are shown for the HMXBs for both galaxies. For the Milky Way the distribution is compiled from the catalog of Liu et al. (2000). For the SMC the distribution is compiled from Table 5. The distributions are normalized to the

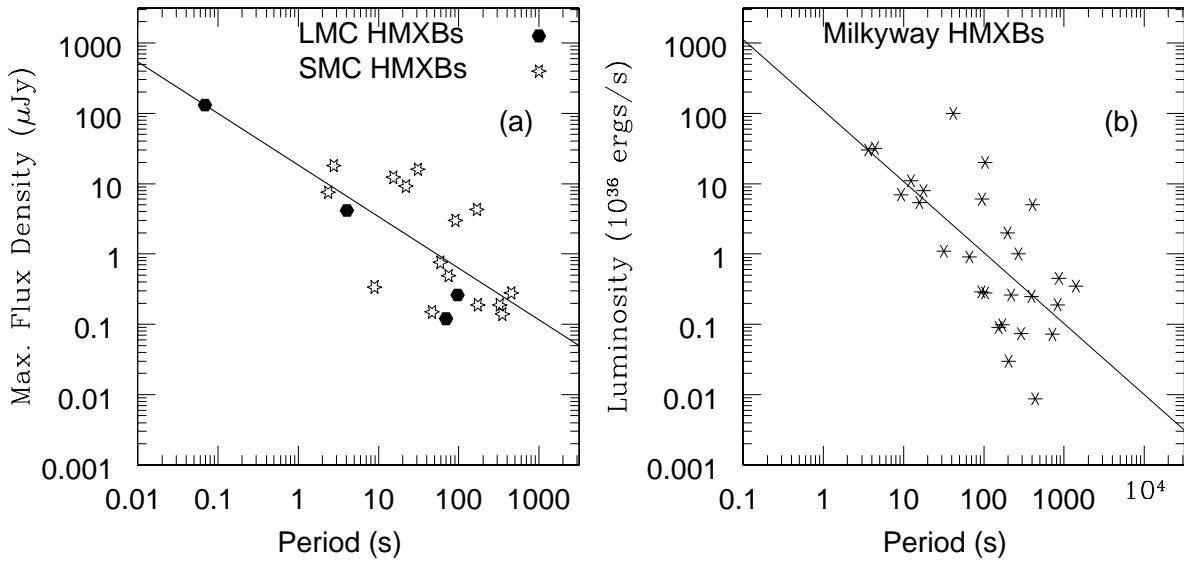


Fig. 8.— a)Maximum flux density versus pulse period for the Be HMXB pulsars of the SMC and LMC. The flux densities of the 4 LMC Be HMXBs have been scaled to the distance of the SMC. The solid line is a least square fit to the 19 data points with a slope of -0.73 ± 0.16 . The correlation coefficient of these data is -0.75 with a probability that it occurs by chance of 2×10^{-4} . b) The Milky Way Be HMXB pulsars from Haberl & Sasaki (2000). The solid line is a fit to the 27 data points with a slope of -1.01 ± 0.21 . The correlation coefficient for these data is -0.69 with a probability that it occurs by chance of 6×10^{-5} .

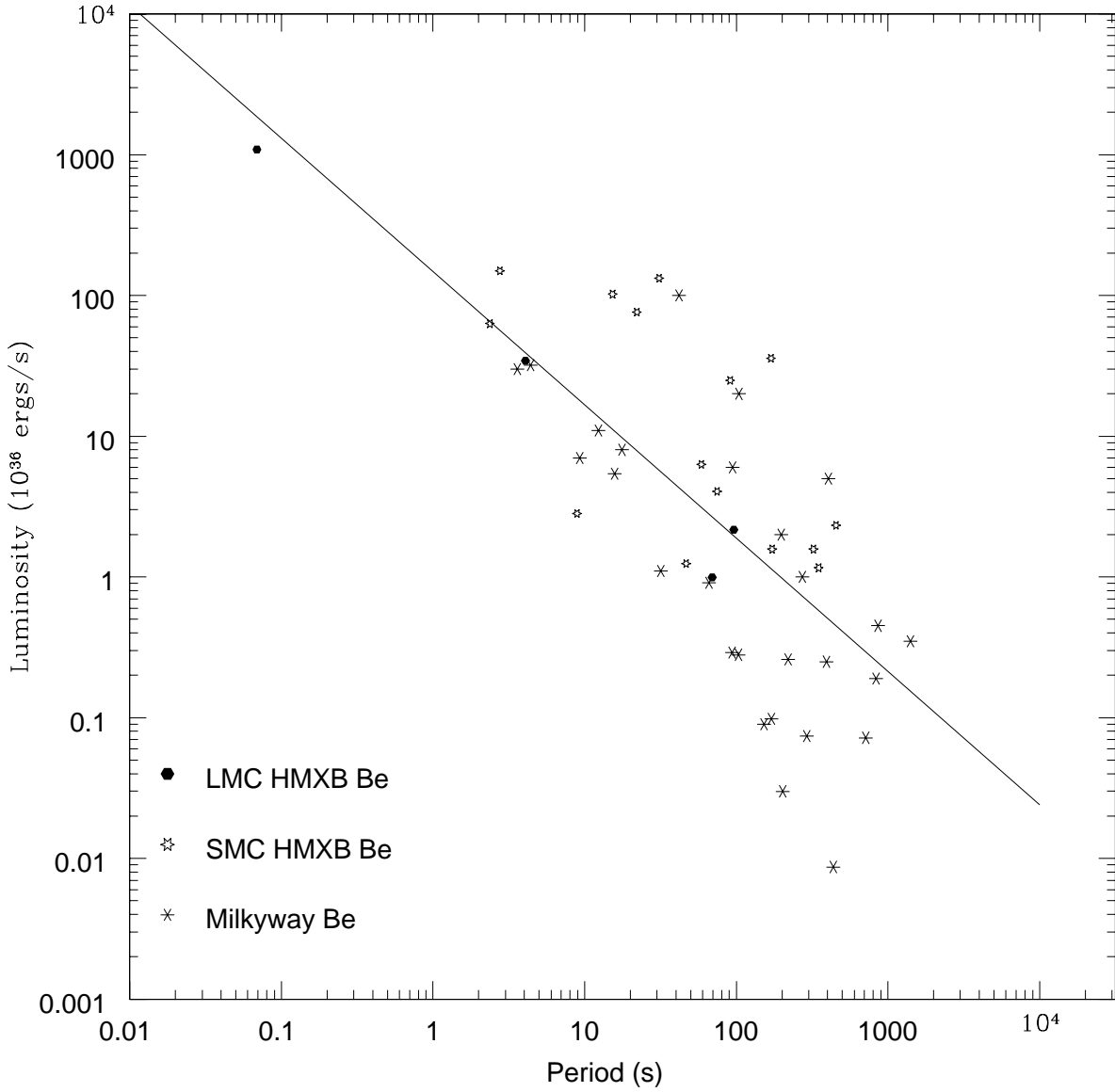


Fig. 9.— Maximum X-ray luminosity for 46 Be HMXB pulsars of the Milky Way, LMC and SMC. For the Magellanic Cloud pulsars the luminosity is for the interval 2-10 keV, an interval believed comparable the intervals for the data of the Milky Way (Haberl & Sasaki 2000). The pulsar data of the Magellanic Clouds has been scaled to an SMC distance of 60 kpc. The correlation has a probability of occurring by chance of 2.9×10^{-8} . The line, a fit to the data points, has a slope -0.95 ± 0.14 .

total number of HMXBs of each kind. The two distributions are virtually identical for periods less than 200 s, however for longer periods there is a slight deficit of SMC HMXBs relative to the Milky Way. If the SMC population is indeed younger than the Milky Way population, a preference for short-period pulsars in the SMC could be construed as evidence that high-mass binaries spin-down over time on average. Since our data does not currently support such a difference, the interpretation is that significant changes of pulse period distributions occur only over timescales longer than the difference in average age between the SMC and Milky Way populations. (This discussion will need to be amended if a significant number of the pulsars in Table 6 should turn out to be HMXBs, since their periods are predominately short period. For example, 12 of the 14 pulsars in Table 6 have periods less than 100s, whereas only 11 of 24 of the pulsars in Table 5 have periods less than 100s.) The slight deficit of long period SMC pulsars seen in Figure 10 may be due to their relative faintness compared to their more rapidly spinning cousins (see Figure 8(a)). This argues for even deeper surveys of the SMC to establish a complete catalog of such objects.

Helpful comments on the manuscript and insight into the accretion process have been made by T. A. Prince. This work made use of software and data provided by the High-Energy Astrophysics Archival Research Center (HEASARC) located at Goddard Space Flight Center, as well as SAS data analysis software from the the XMM-Newton team. Additional use was made of the SIMBAD catalogue at CDS, Strasbourg France, and NASA’s Astrophysics Data System (ADS). This research was carried out at Caltech, Boise State University and the Jet Propulsion Laboratory and supported by the Jet Propulsion Laboratory, California Institute of Technology, under a contract with the National Aeronautics and Space Administration. .

REFERENCES

Allen’s Astrophysical Quantities, 4th edition, A.N.Cox editor, Springer-Verlag New York

Corbet, R. 1986, A & A, 141, 91

Corbet, R., Marshall, F.E. & Markwardt, C.B. 2001, IAUC 7562

Corbet, R., Markwardt, C.B., Marshall, F.E., Laycock, S. & Coe, M.J. 2002, IAUC 7932

Corbet, R., Marshall, F.E., Coe, M.J., Edge, W.R.T. 2003a, IAUC 8064

Corbet, R., Markwardt. C.B., Marshall, F.E., Coe, M.J. & Edge, W.R.T. 2003b, ATEL #163

Corbet, R. et al. 2003c, AAS/HEAD 35, 17.30

Dolphin, A.E., Walker, A.R., Hodge, P.W., Mateo, M., Olszewski, E.W., Schommer, R.A. & Suntzeff, N.B., 2001, ApJ, 562, 202

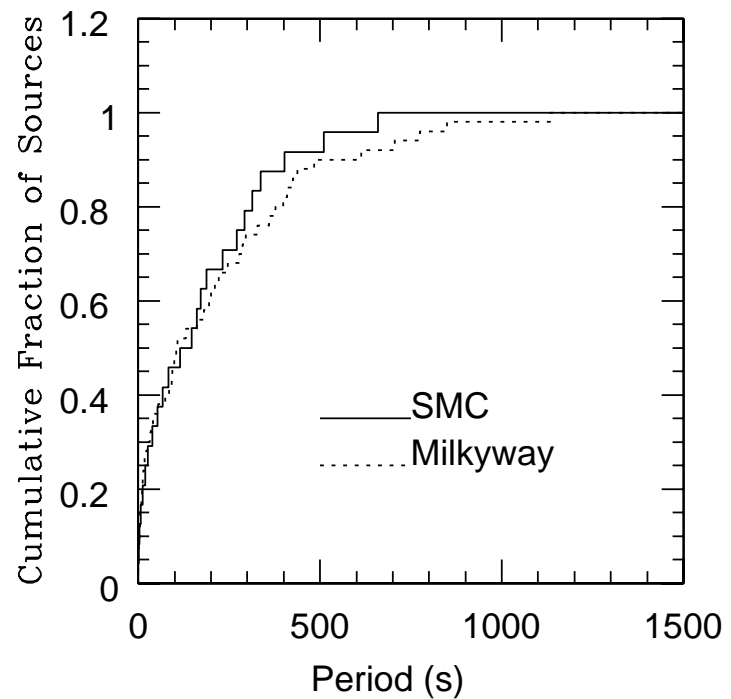


Fig. 10.— Pulse period distributions for the Milky Way and Small Magellanic Cloud high-mass X-ray binary populations. The two distributions are virtually identical for periods less than 200 s, however for longer periods there is a slight deficit of SMC HMXBs relative to the Milky Way.

Finger, M.H., Macomb, D.J., Lamb, R.C., Prince, T.A., Coe, M.J. & Haigh, N.J. 2001, ApJ, 560, 378

Grimm, H.-J., Gilfanov, M. & Sunyaev, R. 2003, MNRAS, 339, 793

Haberl, F. & Sasaki, M. 2000, A&A, 359, 573

Haberl, F. & Pietsch, W. 2004, A&A, in press

Hill, R.J., Madore, B.F. & Freedman, W.L. 1994, ApJ, 429, 192

Imanishi, K., Yokogawa, J. & Koyama, K. 1998, IAUC 7040

Lamb, R.C., Macomb, D.J., Prince, T.A. & Majid, W.A. 2002a, ApJL, 567, 129

Lamb, R.C., Fox, D.W., Macomb, D.J. Prince, T.A. 2002b, ApJ, 574, L29

Lamb, R.C., Prince, T.A., Macomb, D.J. & Majid, W.A. 2003, IAUC 8220

Laycock, S., Corbet, R.H.D., Perrodin, D., Coe, M.J., Marshall, F.E. Markwardt, C. 2002, A&A, 385, 464

Liu, Q.Z., van Paradijs, J. & van den Heuvel, E.P.J. 2000, A&A, 363, 660

Macomb, D.J., Finger, M.H., Harmon, B.A., Lamb, R.C. & Prince, T.A. 1999, ApJ, 518, L99

Macomb, D.J., Fox, D.W., Lamb, R.C. & Prince, T.A. 2003, ApJ, 584, L79

Mereghetti, S., Chiarlone, L., Israel, G.L. & Stella, L. 2002, Proceedings of the 270. WE-Heraeus Seminar on Neutron Stars, Pulsars, and Supernov Remnants. MPE Report 278. p. 29

Maragoudaki, F. et al. 2001 A&A, 379, 864

Sasaki, M., Pietsch, W. & Haberl, F. 2003, A&A, 403, 901

Strüder, L. et al. 2001, A&A, 365, L18

Turner, M.J.L. et al. 2001, A&A, 365, L27

Udalski, A. Szymanski, M., Kubiak, M. Pietrzynski, G., Wozniak, P. & Zebrun, K. 1998, Acta Astron., 48, 147

Verbunt, F. & van den Heuvel 1996, p. 457 in X-ray Binaries. ed. Lewin, W.H.G., van Paradijs, J. & van den Hevel, E.P.J. 1996 Cambridge University Press

Waters, L.B.F.M & van Kerkwijk, M.H. 1989, A&A, 223, 196

Yokogawa, J. & Koyama, K. 1998, IAUC 7028

Yokogawa, J. & Koyama, K. 2000, IAUC 7361

Yokogawa, J. et al. 2000, PASJ, 52, 53

Yokogawa, J., Imanishi, K., Tsujimoto, M., & Koyama, K. 2003, PASJ, 55, 161

Zaritsky, D., Harris, J., Thompson, I.B., Grebel, E.K. & Massey, P. 2002, AJ, 123, 855